Holding the balance; the equilibrium between ERα-activation, epigenetic alterations and chromatin integrity

Flach, K.D.

Chapter 6

ERα Cofactor phosphorylation

SRC3 phosphorylation at Serine 543 is a positive independent prognostic factor in ER positive breast cancer

Koen D. Flach[1*], Wilbert Zwart[1*], Bharath Rudraraju[2*], Tarek M.A. Abdel-Fatah[3], Ondrej Gojis[4], Sander Canisius[1], David Moore[5], Ekaterina Nevedomskaya[1], Mark Opdam[1], Marjolein Droog[1], Ingrid Hofland[1], Steve Chan[4], Jacqui Shaw[5], Ian O. Ellis[6], R. Charles Coombes[3], Jason S. Carroll[7], Simak Ali[3], and Carlo Palmieri[2,8,9]

[*]Authors contributed equally
[1]Department of Molecular Pathology, The Netherlands Cancer Institute, Amsterdam, the Netherlands.
[2]Department of Molecular and Clinical Cancer Medicine, Institute of Translational Medicine, The University of Liverpool, Liverpool, UK.
[3]Clinical Oncology Department, Nottingham University City Hospital NHS Trust, Nottingham, UK.
[4]Cancer Research UK Laboratories, Imperial Centre for Translational and Experimental Medicine, Division of Cancer, Imperial College London, London, UK.
[5]Department of Cancer Studies and Molecular Medicine, University of Leicester, Leicester, UK.
[6]Division of Pathology, School of Molecular Medical Sciences, University of Nottingham, Nottingham, UK.
[7]Cancer Research UK Cambridge Institute, Cambridge, UK.
[8]Liverpool and Merseyside Academic Breast Unit, The Linda McCartney Centre, Royal Liverpool University Hospital, Liverpool, UK.
[9]Academic Department of Medical Oncology, Clatterbridge Cancer Centre NHS Foundation Trust,Wirral, UK.

Clin Cancer Res. 2016 Jan 15;22(2):479-91

Abstract

Purpose: The steroid receptor coactivator SRC3 is essential for the transcriptional activity of estrogen receptor α (ERα). SRC3 is sufficient to cause mammary tumorigenesis, and has also been implicated in endocrine resistance. SRC3 is posttranslationally modified by phosphorylation, but these events have not been investigated with regard to functionality or disease association. Here, we investigate the spatial selectivity of SRC3-pS543/DNA binding over the human genome and its expression in primary human breast cancer in relation with outcome.

Experimental Design: Chromatin immunoprecipitation, coupled with sequencing, was used to determine the chromatin binding patterns of SRC3-pS543 in the breast cancer cell line MCF7 and two untreated primary breast cancers. IHC was used to assess the expression of SRC3 and SRC3-pS543 in 1,650 primary breast cancers. The relationship between the expression of SRC3 and SRC3-pS543, disease-free survival (DFS), and breast cancer specific survival (BCSS) was assessed.

Results: Although total SRC3 is selectively found at enhancer regions, SRC3-pS543 is recruited to promoters of ERα responsive genes, both in the MCF7 cell line and primary breast tumor specimens. SRC3-pS543 was associated with both improved DFS ($P = 0.003$) and BCSS ($P = 0.001$) in tamoxifen untreated high-risk patients, such a correlation was not seen in tamoxifen-treated cases, the interaction was statistically significant ($P = 0.001$). Multivariate analysis showed SRC3-pS543 to be an independent prognostic factor.

Conclusions: Phosphorylation of SRC3 at S543 affects its genomic interactions on a genome-wide level, where SRC3-pS543 is selectively recruited to promoters of ERα-responsive genes. SRC3-pS543 is a prognostic marker, and a predictive marker of response to endocrine therapy. Clin Cancer Res; 22(2); 479–91. ©2015 AACR.

Translational Relevance: SRC3 is an essential coactivator for the transcriptional activity of ERα and is required for estrogen-dependent cell proliferation. Analogous to ERα, SRC3 is typically found at enhancer regions involved in long-range regulation of hormonal-responsive genes. In this study, we establish the genome-wide chromatin binding preferences for activated SRC3 (SRC3-pS543) in ERα-positive breast cancer, as well as the association

between SRC3-pS543 expression and clinicopathologic features and clinical outcomes in 1,650 primary breast cancers. Our findings reveal that while ERα and total SRC3 are predominately found in distal enhancers and introns, SRC3-pS543 is predominately located at promoters of genes. SRC3-pS543 was associated with favorable clinicopathologic features and was found to be an independent prognostic factor as well as a predictive marker with regard to tamoxifen treatment. These observations illustrate that high expression of SRC3-pS543 can potentially identify a population of early ER-positive breast cancer with a good clinical outcome without receiving adjuvant therapy.

Introduction

Estrogen receptor α (ERα) is a key transcription factor in normal breast development and plays a central role in the pathogenesis of approximately 70% of all breast cancers. Consequently, ERα is recognized as the key therapeutic target in this group of patients (1). The p160 steroid receptor coactivator (SRC) family member, SRC3 (also known as amplified in breast cancer 1; AIB1) is an essential coactivator for the transcriptional activity of ERα, which recruits SRC3 to chromatin (2). SRC3 is required for estrogen-driven proliferation of MCF7 breast cancer cells (3) and is critical for normal mammary development (3). Overexpression of SRC3 can induce mammary tumorigenesis in mice (4), while its absence protects against breast cancer development (5, 6). SRC3 was originally identified as a gene mapping to a region of chromosome 20 (20q12–13), which is frequently amplified in breast cancer and was shown to be amplified in 10% of breast cancers (7). SRC3 mRNA levels are significantly higher in breast cancer as compared with normal mammary tissue (8, 9) and SRC3 protein levels are elevated in 16% to 83% (depending on the study) of human breast tumors (10).

SRC3 expression has been associated with decreased risk of relapse in patients with breast cancer who did not receive adjuvant endocrine therapy (11). Conversely, in tamoxifen-treated patients SRC3 expression was associated with poor outcome and increased risk of relapse (11). Others have found no such association with tamoxifen treatment, although an increased risk was seen with high SRC3 when expressed alongside HER1, HER2, or HER3 (12). In a group of women of whom 82% were postmenopausal, SRC3 expression has been associated with early recurrence on tamoxifen treatment (13), although high SRC3 in premenopausal women was an independent predictive factor of improved response to tamoxifen (14). ERα-associated SRC3 is typically found at enhancer regions, where expression of genes proximal

to shared ERα/SRC3 chromatin binding events correlates with poor outcome of ERα-positive patients with breast cancer treated with tamoxifen (15). This feature was only found for genes where SRC3 was selectively enriched as compared with the other two p160 family members, SRC1 and SRC2.

Phosphorylation of SRC3 is required for it to function as a potent transcriptional activator, and SRC3 possesses multiple phosphorylation sites that may be functionally involved in this process (16, 17). Estradiol treatment increases SRC3 phosphorylation, but the kinase responsible for this remains elusive. However, a number of kinases are known that induce phosphorylation at these residues of SRC3 (16, 17). In addition, dephosphorylation of serine-101 and -102 regulates SRC3 protein stability by preventing proteasome-dependent turnover (18). Of note, the C-terminal domain of SRC3 has weak histone acetyltransferase activity raising the possibility that it may have a role in chromatin remodeling (10).

Previous studies have shown a requirement of SRC3 phosphorylation for SRC3 activity, including phosphorylation of SRC3 at serine residue 543 (SRC3-pS543 (16)). Furthermore, the region around S543 is evolutionarily conserved in mammals, birds, and reptiles, although no sequence homology around S543 is found in SRC1 or SRC2 (19). In addition, thus far no studies explored the genomic consequences and clinical significance of SRC3 phosphorylation. Given all the above, we decided to investigate the chromatin associations of SRC3 in vitro and in vivo when phosphorylated at serine 543 (SRC3-pS543) together with its clinical significance in ERα-positive breast cancer. To separate the prognostic from the predictive potential of SRC3 phosphorylation, tamoxifen-treated patients were compared with patients who did not receive any adjuvant endocrine therapy.

Results

Specificity of SRC3-pS543 antibody

An antibody for SRC3-pS543 was generated, which recognized wild-type phosphorylated SRC3, but not S543-mutated SRC3 (S543A; **Fig. 1A**). The SRC3-pS543 antibody detected SRC3 in immunoprecipitates from MCF7 cell lysates (**Fig. 1A and B**; full size blot Supplementary Figs. S1 and S2), where signal was lost after the phosphatase treatment (**Fig. 1B**). Consistent with a previous report (17), we find estrogen treatment to increase S543 phopshorylation in a dose-dependent manner, further validating our SRC3-pS543 antibody (**Fig. 1C**). To ensure the specificity of the SRC3-pS543 antibody

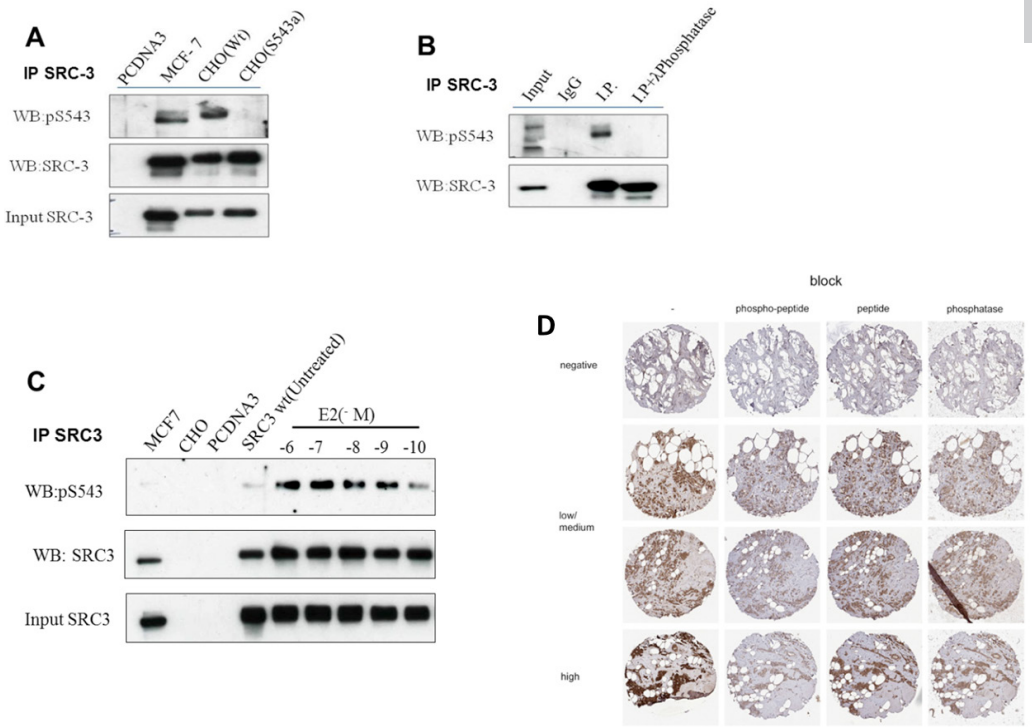

Figure 1: *Validation of phosphostate-specific antibody.*
(A) CHO cells were transfected with pCDNA3, Flag-tagged wild-type (WT) SRC3 or a Flag-tagged SRC3 mutant in which serine at residue 543 has been substituted by alanine. MCF7 cells were used as control. The lysates were immunoprecipitated with SRC-3 antibody. Immunoblotting was performed for SRC-3 and phospho-S543. Note that the Flag-tagged SRC3 migrates slower on Western blot as compared with endogenous SRC3. (B) MCF7 cell lysate was immunoprecipated with SRC-3 antibody. The beads were then divided into two halves, one untreated and the other treated with λ-phosphatase. Immunoblotting was performed for SRC-3 and phosphorylation state-specific antibody. (C) CHO cells were grown in DMEM with dextran-coated charcoal stripped FCS for 72 hours and then transfected with vector (pCDNA3) or SRC-3 for 24 hours. Cells were then treated with vehicle or increasing concentrations of 17β-estradiol (E2) for 1 hour before making lysates for immunoprecipitation. Western blotting was carried out with the antibodies indicated. MCF7 cells were used as control. (D) Representative tumor sections following preincubation with phospho-peptide and nonphospho-peptide and phosphatase treatment prior to staining with SRC3-pS543 in breast cancers with negative, low/medium, and high expression of SRC3-pS543.

by IHC, the antibody was incubated with either peptide containing the phospho-moiety or the nonphospho-peptide. Subsequently, the preincubated antibody (bound to nonphospho-peptide and phospho-peptide) was tested on four tumors with different levels of signal for SRC3-pS543 (negative, low/medium, and high; **Fig. 1D**). In addition, phosphatase treatment was applied. Although the phospho-peptide strongly decreased pS543-SRC3 signal, this was not observed with the nonphospho-peptide. In addition, phosphatase treatment strongly diminished pS543-SRC3 signal in all tested specimens (**Fig. 1D**).

ChIP-seq analysis shows a genomic preference of SRC3-pS543 to bind promoter regions

Next, we determined the genome-wide distributions of this SRC3-pS543 phosphorylation as compared with total SRC3 and ERα in asynchronously proliferating luminal breast cancer cells MCF7 as exemplified for well-known ERα binding sites proximal to the XBP-1 locus (**Fig. 2A**). For ERα genomic locations, data from ref. 24 were used, although total SRC3 data were from ref. 15. In total, 47,214 ERα binding sites were detected, of which 15,329 were also bound by SRC3 (ref. 15; **Fig. 2B**). Between ERα, SRC3, and SRC3-pS543, 2,365 peaks were shared (for raw data visualizations, see **Fig. 2C**). Not all SRC3 binding events were phosphorylated and 2,795 peaks for SRC3-pS543 were apparently not shared with total SRC3. However, there was weak total SRC3 signal observed at these positions, which did not reach the detection threshold for peak calling (Supplementary Fig. S3A and S3B). Based on these results, we conclude that differential binding patterns between SRC3-pS543 and total SRC3 should be considered as "enriched" rather than "unique." P160 family members share substantial sequence homology. Even though the sequence surrounding S543 is not conserved in SRC1 and SRC2, the SRC3-pS543 antibody might still detect the other two p160 members. Therefore, we determined potential overlap of SRC3-pS543 enriched sites with SRC1 and SRC2 in MCF7 cells (15). The overlap of SRC3-pS543 enriched sites with SRC1 and SRC2 was limited, rendering it unlikely that the SRC3-pS543 enriched sites can be explained merely by cross-reactivity with one of the other p160s (Supplementary Fig. S4). Differential chromatin binding between SRC3-pS543 and total SRC3 could be validated by qPCR analyses on asynchronous MCF7 cells (Supplementary Fig. S5A), using four primer sets that were designed for each subset of binding sites, that is, SRC3-pS543-enriched, total SRC3-enriched, and shared sites (Supplementary Table S1 for

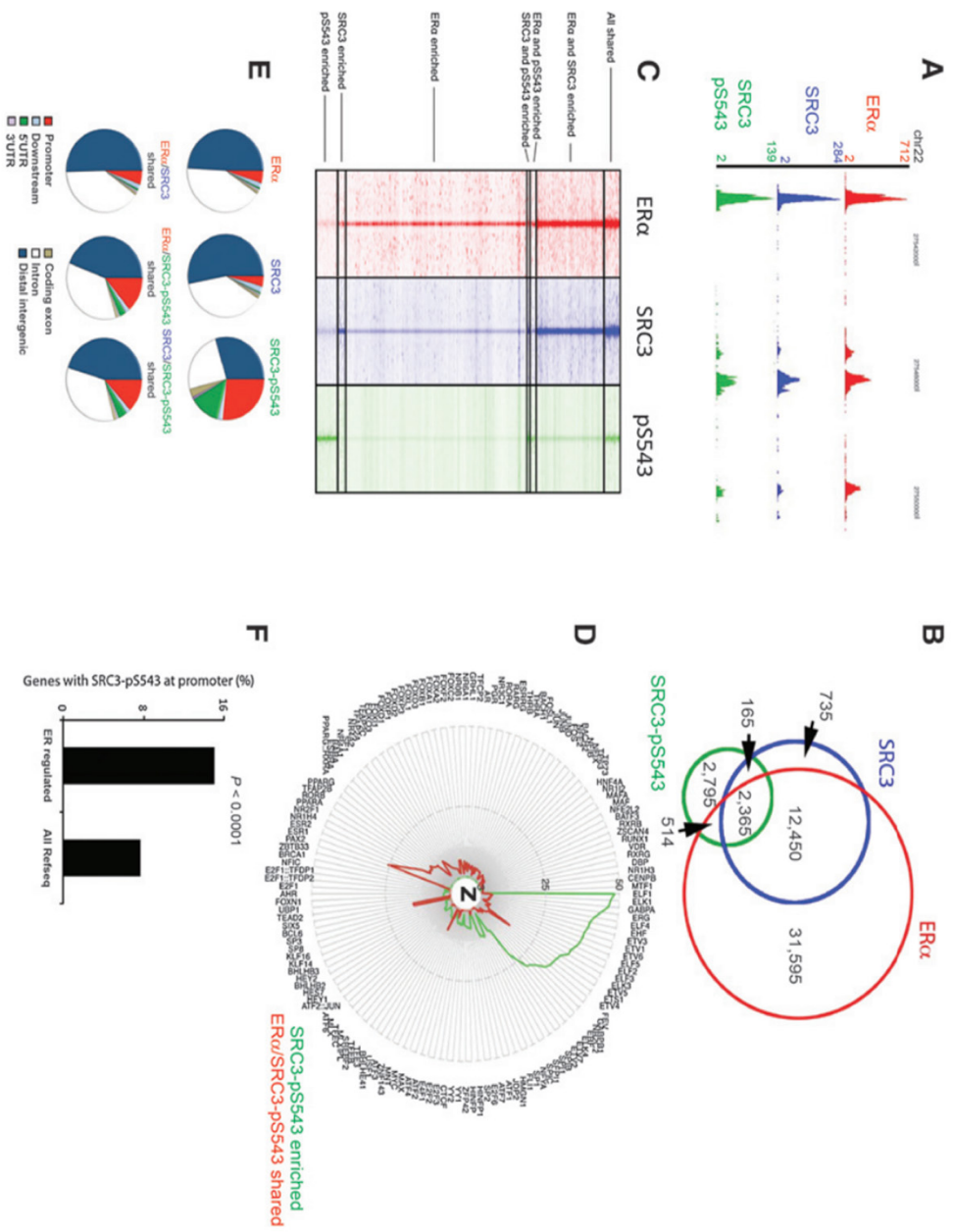

Figure 2*: SRC3-pS543, SRC3, and ERα chromatin binding patterns in MCF7 cells. (A) Genome browser snapshot of ChIP-seq samples for ERα (red), SRC3 (blue), and SRC3-pS543 (green) in proliferating MCF7 cells. Y bar shows tag count. Genomic*

coordinates are indicated. (B) Venn diagram of ERα (red), SRC3 (blue), and SRC3-pS543 (green). Numbers of shared and unique peaks are shown. (C) Heatmap visualization of ERα (red), SRC3 (blue), and SRC3-pS543 (green). (D) Motif analyses of ERα/SRC3-pS543 shared and SRC3-pS543 enriched binding sites. Z-score for each motif is shown in a MRP. Motif enrichment is shown for chromatin binding sites shared between ERα and SRC3-pS543 (red) or selectively enriched for SRC3-pS543 (green). The radial data points represent the absolute value of Z-score. (E) Genomic distributions of ERα, SRC3, and SRC3-pS543 sites. (F) Percentage of ERα-regulated genes with a SRC3-pS543 binding event at the promoter, compared with all refseq genes. $\chi 2$ test: $P < 0.0001$.

primer sequences and Supplementary Fig. S5B for genome browser snapshots of SRC3 and SRC3-pS543 ChIP-seq signal at these sites). To assess hormone dependency of SRC3-pS543 chromatin interactions, SRC3-pS543 ChIP-qPCR was performed on cells that were hormone deprived for 3 days, and subsequently treated for 3 hours with vehicle, E2, or tamoxifen (Supplementary Fig. S6). SRC3-pS543/chromatin interactions at SRC3-pS543-enriched sites (that were not bound by ERα) were hormone independent and not affected by ligand. For SRC3-pS543 sites shared with total SRC3, no chromatin binding was observed in the absence of hormone and in tamoxifen-treated cells, but this interaction was actively induced by E2 treatment. Phosphatase treatment abrogated SRC3-pS543 enrichment at these sites (Supplementary Fig. S6). Genomic distributions of ERα and SRC3 were comparable as reported by others (ref. 29; Supplementary Fig. S7). To further illustrate functional interplay between ERα and SRC3-pS543, ERα was depleted from MCF7 cells using Fulvestrant (Supplementary Fig. S6). SRC3-pS543/SRC3 shared, but not SRC3-pS543-enriched chromatin interactions were dependent on ERα levels, as shown by Fulvestrant-mediated ERα degradation (Supplementary Fig. S8). In order to identify potential selectivity of transcription factor usage, motif analyses were performed on the sites that were either or not shared between SRC3-pS543 and ERα, and visualized in a MRP (**Fig. 2D**). For the shared events, motif enrichment was found for classical luminal breast cancer–selective transcription factors, including ESR1 and forkhead motifs. For SRC3-pS543-enriched binding events, no motifs for ESR1 or FOXA1 were enriched, but a clear enrichment was observed for ELK, ELF, and ETV motifs (see also Supplementary Table S4 for the total list).

Differential motif enrichment could form the basis of differential gene expression programs. Therefore, GO pathway enrichment was assessed

for genes with an SRC3/chromatin binding event proximal (<20 kb) to their transcription start sites. GO terms highly varied for the differential SRC3 subclasses (Supplementary Fig. S9), with 1 out of 80 GO terms for SRC3 enriched sites ("biologic process") shared with the other two subsets. Interestingly, the majority of SRC3-pS543/SRC3 shared peak GO terms, 28 out of 37, were overlapping with those found for the SRC3-pS543-enriched sites, including "metabolic process," "gene expression," and "translation." For a complete list of all GO terms, see Supplementary Table S5.

Because the SRC3-pS543 chromatin binding events only recapitulated a proportion of the total SRC3 binding events, genomic distributions could deviate as well. As described before (15, 30), the majority of ERα and SRC3 binding events are found within enhancers and introns (**Fig. 2E**). In contrast, SRC3-pS543 binding was clearly enriched at promoter regions and 5′UTR, with promoter-bound SRC3-pS543 colocalizing with SRC3, ERα, and histone modifications indicative for active gene transcription (H3K4me2, H3K4me3, and H3K27Ac; Supplementary Fig. S10). As expected, SRC3 and ERα signal was found centered on the SRC3-pS543 signal. Because transcription factors bind accessible chromatin, histone marks indicative for active promoters (H3K4me3 and H3K27Ac) are found around the SRC3-pS543 sites instead of directly centered on them. Interestingly, this was not the case for H3K4me2, which was clearly enriched on the SRC3-pS543 peak. The enhancer-selective histone mark H3K4me1 was not enriched at SRC3-pS543 promoters. Even though less pronounced than the total of SRC3-pS543 peaks, the sites shared between ERα and SRC3-pS543 were also more promoter enriched (13.9%) as compared with the ERα/SRC3 shared regions (4.9%). Furthermore, SRC3-pS543 signal was highly enriched at promoters of E2-regulated genes (31) as compared with all Refseq genes ($P < 0.0001$; **Fig. 2F**).

SRC3-pS543 and ERα chromatin binding events in primary tumor tissue

Next, we determined phosphorylated SRC3/chromatin interactions in primary tumors (**Fig. 3**). ChIP-seq was performed on two independent ER+/PR+/HER2− breast tumor specimens as described (21, 24), and directly compared with the MCF7 cell line data. Peak intensities between the two tumors and the MCF7 sample were comparable, and peaks are well conserved (**Fig. 3A**). Between the two tumors and MCF7 cells, 2,670 binding events of SRC3-pS543 were shared (**Fig. 3B**, visualized in a raw heatmap in **Fig. 3C**). Furthermore, peaks were also found selectively enriched for only MCF7 (2,523 sites), tumor #1 (1,816 sites), or tumor #2 (4,631 sites). The SRC3-pS543 binding

sites from all samples were annotated for their genomic distributions, and again enrichment for promoters and 5′UTR regions was found (**Fig. 3D**). This was even more strikingly observed for binding events shared by all three samples, with 52% of all sites being localized to promoters and 20% at 5′UTR. For tumor #1, the lysate was divided in two prior to immunoprecipitation, and the second half of the lysate was used for ERα ChIP-seq, enabling a direct comparison of SRC3-pS543 and ERα binding patterns within the same tumor (**Fig. 3E**). Between ERα and SRC3-pS543, 1,727 binding events were shared, although 15,050 binding events were only found for ERα and 5,537 binding sites were only found for SRC3-pS543 (**Fig. 3F**). The shared and enriched binding patterns were not dictated by different thresholds in peak calling algorithms, as shown by heatmap analyses (**Fig. 3G**). The genomic distributions of ERα in the tumor sample closely resemble what was found in the cell line (**Fig. 2E**) and previously reported in breast tumor tissue (21, 24), with approximately 5% of ERα binding events being found at promoters, with the vast majority of sites located at distal enhancers and introns (**Fig. 3H**). The SRC3-pS543 sites (either or not shared with ERα), were highly enriched at promoters and 5′UTR regions.

Motif analyses for the ERα binding events in the tumor specimen revealed enrichment in ERα, FOXA1, and AP-2 motifs, as expected (refs. 30, 32; **Fig. 3I**). Enrichment for these specific motifs was found both for ERα-enriched sites as well as for sites shared between ERα and SRC3-pS543. Furthermore, practically all motifs found at SRC3-pS543–enriched sites were also found at the regions shared by ERα and SRC3-pS543 bounds, including motifs for ELK, ETV, and ETS factors as were observed in the MCF7 cells (see Supplementary Table S6 for the total list).

Association of total SRC3 and SRC3-pS543 with clinicopathologic features

Total SRC3 and SRC3-pS543 expression was evaluated in 1,650 breast carcinomas, with protein expression predominately nuclear (Supplementary Fig. S11). The total SRC3 mean histoscore was 157 (interquartile range, 0–300) and for SRC3-pS543 mean histoscore was 31 (interquartile range, 0–300). For subsequent analysis, total SRC3 expression was categorized as high (above mean, H-score > 157) or low (below mean, H-score < 157) and for SRC3-pS543 high (above mean, H-score > 31) or low (below mean, H-score ≤ 30; Supplementary Table S3). A scatterplot analysis of total SRC3 versus SRC3-pS543 in these tumors shows that the relative levels between total SRC3 ver-

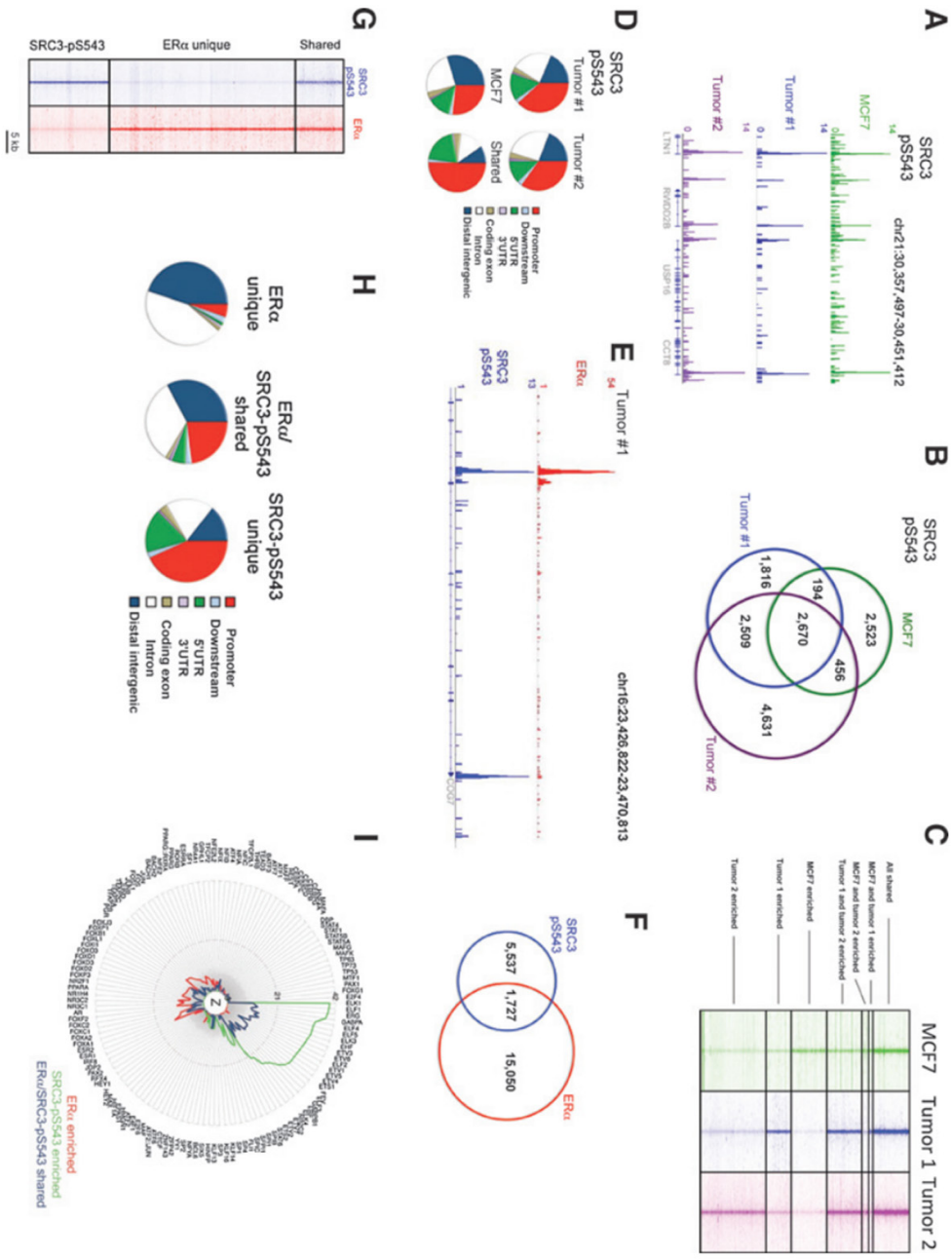

Figure 3: *SRC3-pS543 binding events in MCF7 cells and breast tumors.*
(A) Genome browser snapshot, ChIP-seq for SRC3-pS543 on MCF7 cells (green),

tumor sample #1 (blue), and tumor sample #2 (purple). Y bar shows tag count. Genomic coordinates are indicated. (B) Venn diagram of SRC3-S543P ChIp-seq for MCF7 cells (green), tumor sample #1 (blue), and tumor sample #2 (purple). Number of shared and unique sites is illustrated. (C) Heatmap visualization of SRC3-S543P ChIp-seq for MCF7 cells (green), tumor sample #1 (blue), and tumor sample #2 (purple). Number of shared and enriched sites is illustrated. (D) Genomic distributions of shared and unique SRC3-pS543 binding events for MCF7 cells, tumor sample #1, and tumor sample #2. (E) Genome browser snapshot, ChIP-seq on a primary breast tumor for ERα (red) and SRC3-pS543 (blue). (F) Venn diagram of ERα (red) and SRC3-pS543 (blue) binding events. (G) Heatmap analysis, depicting all shared and enriched binding events for ERα (red) and SRC3-pS543 (blue). Shown are all binding events with a window of 5 kb around the binding site. (H) Genomic distributions of the shared and enriched binding events of ERα and SRC3-pS543. (I) Motif analyses of the shared and enriched binding events of ERα and SRC3-pS543. Z-score for each motif is shown in a MRP. Motif enrichment is shown for chromatin binding sites enriched for ERα (red), SRC3-pS543 (green), or shared between ERα and SRC3-pS543 (blue). The radial data points represent the absolute value of Z-score.

sus SRC3-pS543 were strongly variable between tumors. Most importantly, a large proportion of tumors were identified that were positive for total SRC3, but negative for SRC3-pS543. Furthermore, no tumors could be identified that were positive for the phospho-SRC3 but negative for total SRC3, again highlighting specificity of the antibody (Supplementary Fig. S12).

Although no association on IHC between total SRC3 and ERα was found, there was a strong association for SRC3-pS543 with ERα ($P = < 0.0001$) and high expression of ERα-associated proteins (progesterone receptor; $P = < 0.0001$ and Bcl2; $P = < 0.0001$). Total SRC3 expression was significantly associated with HER2 ($P = < 0.0001$) and HER3 ($P = 0.023$), and correlated the absence of basal-like ($P = 0.021$) and triple negative phenotypes ($P = 0.005$; Table 1). SRC3-pS543 was significantly associated with well-differentiated ($P \leq 0.0001$), low proliferative ($P \leq 0.0001$) tumors, as well as androgen receptor ($P \leq 0.0001$) expression. In addition, it was associated with the presence of p53 ($P = 0.025$) and the absence of MDM4 ($P < 0.001$) and MDM2 ($P < 0.001$), as well as the absence of both basal-like and triple negative phenotypes ($P < 0.0001$). The absence of SRC3-pS543 was significantly associated with the overexpression of HER4 ($P < 0.0001$), the presence of lympho-vascular invasion ($P \leq 0.0001$), and loss of expression of the key DNA repair proteins, including BRCA1 ($P < 0.0001$), ATM ($P <$

0.0001), and TOP2A (P < 0.0001; Table 1). Apart from being phosphorylated by estrogen treatment, SRC3-S543 is also phosphorylated by JNK and p38 MAPK (16). In line with these previous observations, we find a significant correlation between the phosphorylated JNK and p38 MAPK with SRC3-pS543 (P < 0.0001; Table 1). Additional tumor biomarkers and their correlation with SRC3 and SRC3-pS543 are shown in Supplementary Table S7.

Association of total SRC3 and SRC3-pS543 expression with outcome

With regard to outcome, no association of total SRC3 with outcome was observed in the whole cohort (Supplementary Fig. S11A), the ERα-positive group in total (Supplementary Fig. S11B), or on the basis of tamoxifen treatment (Supplementary Fig. S11D–S11F). Furthermore, no association of total SRC3 with outcome was observed in the ERα-negative cohort (Supplementary Fig. S11C). However, expression of SRC3-pS543 in the whole cohort was associated with significantly longer disease-free survival (DFS) (P < 0.00001) and breast cancer specific survival (BCSS) (P = 0.0001; **Fig. 4A**). SRC3-pS543 expression in the ERα-positive cohort correlated with a longer DFS (P = 0.003) and BCSS (P = 0.001; **Fig. 4B**), although SRC3-pS543 did not associate with survival in ERα-negative breast cancers (**Fig. 4C**). Furthermore, in low-risk ERα-positive cancers, no correlation of SRC3-pS543 with outcome was found (**Fig. 4D**).

Importantly, SRC3-pS543 was associated with a longer DFS (P = 0.035) and BCSS (P = 0.005) in ER-positive high-risk breast cancer not treated with tamoxifen (**Fig. 4E**). In high-risk patients who did receive tamoxifen, SRC3-pS543 did not associate with a longer DFS (P = 0.57) or BCSS (P = 0.21; **Fig. 4F**). For ER-positive high-risk patients with low SRC3-pS543, exposure to tamoxifen reduced the risk of death from breast cancer [HR (95% CI) = 0.68 (0.49–0.94), P = 0.019] by 32% (**Fig. 4G**), whereas for those with high pS543, there was no effect (**Fig. 4H**), the interaction was statistically significant (P = 0.001). Similarly, exposure to tamoxifen reduced risk of recurrence by 42% [HR (95% CI) = 0.58 (0.44–0.77), P = 0.0001] in ER+ high-risk patients with low pS543, whereas no effect on those with high pS543 patients, the interaction was statistically significant (P = 0.000.1). Tamoxifen-treated patients with HER2-positive tumors that expressed high levels of SRC3 had a significantly shorter disease-free and BCSS. This was not observed for the patients who did not receive endocrine treatment (Supplementary Fig. S14).
SRC3-pS543 was confirmed as an independent prognostic factor in breast cancers after adjustment for endocrine therapy and other validated prognostic

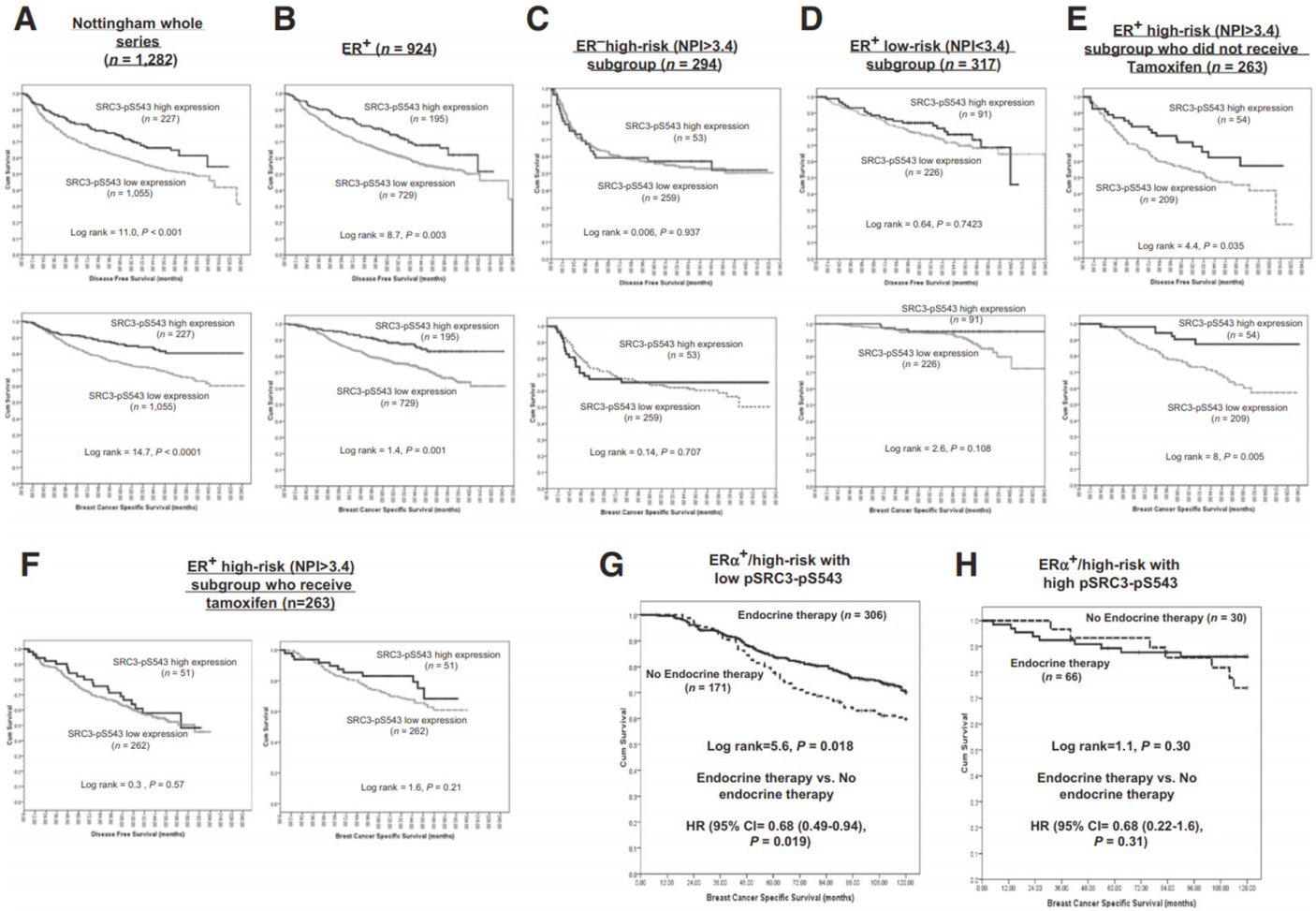
A
Nottingham whole series (n = 1,282)
SRC3-pS543 high expression (n = 227)
SRC3-pS543 low expression (n = 1,055)
Log rank = 11.0, P < 0.001
Log rank = 14.7, P < 0.0001
B
ER+ (n = 924)
SRC3-pS543 high expression (n = 195)
SRC3-pS543 low expression (n = 729)
Log rank = 8.7, P = 0.003
Log rank = 1.4, P = 0.001
C
ER−high-risk (NPI>3.4) subgroup (n = 294)
SRC3-pS543 high expression (n = 53)
SRC3-pS543 low expression (n = 259)
Log rank = 0.006, P = 0.937
Log rank = 0.14, P = 0.707
D
ER+ low-risk (NPI<3.4) subgroup (n = 317)
SRC3-pS543 high expression (n = 91)
SRC3-pS543 low expression (n = 226)
Log rank = 0.64, P = 0.7423
Log rank = 2.6, P = 0.108
E
ER+ high-risk (NPI>3.4) subgroup who did not receive Tamoxifen (n = 263)
SRC3-pS543 high expression (n = 54)
SRC3-pS543 low expression (n = 209)
Log rank = 4.4, P = 0.035
Log rank = 8, P = 0.005
F
ER+ high-risk (NPI>3.4) subgroup who receive tamoxifen (n=263)
SRC3-pS543 high expression (n = 51)
SRC3-pS543 low expression (n = 262)
Log rank = 0.3 , P = 0.57
Log rank = 1.6, P = 0.21
G
ERα+/high-risk with low pSRC3-pS543
Endocrine therapy (n = 306)
No Endocrine therapy (n = 171)
Log rank=5.6, P = 0.018
Endocrine therapy vs. No endocrine therapy
HR (95% CI= 0.68 (0.49-0.94), P = 0.019)
H
ERα+/high-risk with high pSRC3-pS543
No Endocrine therapy (n = 30)
Endocrine therapy (n = 66)
Log rank=1.1, P = 0.30
Endocrine therapy vs. No endocrine therapy
HR (95% CI= 0.68 (0.22-1.6), P = 0.31)
Cum Survival
Disease Free Survival (months)
Breast Cancer Specific Survival (months)

Figure 4*: DFS and BCSS in patients with breast cancer based on SRC3-pS543 protein expression.*
(A) Entire Nottingham cohort. (B) ERα-positive cohort. (C) ERα-negative cohort NPI > 3.4. (D) ERα-positive patients NPI < 3.4 who did not receive tamoxifen. (E) ERα-positive patients NPI ≥ 3.4 who did not receive tamoxifen. (F) ERα-positive patients NPI ≥ 3.4 who received tamoxifen. (G) BCSS based on SRC3-pS543 protein expression and tamoxifen treatment in the ERα-positive high-risk group with low pSRC3-pS543. (H) BCSS based on SRC3-pS543 protein expression and tamoxifen treatment in the ERα-positive high-risk group with high pSRC3-pS543.

factors; and absence of SRC3-pS543 signal correlated with recurrence (HR = 1.4, CI 95%, 1.1–2.5) and death from breast cancer (HR = 1.6, CI 95%, 1.1–2.5; Table 2).

Discussion

Coactivators for ERα have been the focus of many clinical and cell biologic studies. SRC3 is of particular interest, because the SRC3 gene is frequently amplified in breast cancer (7), and its expression was found to correlate with HER2 expression levels and poor outcome (11). SRC3 is a member of the p160 coregulator protein family (along with SRC1 and SRC2), which all have shared and preferred genome-wide chromatin binding patterns, which are strongly induced by ERα activation (15).

Here, we focus on one distinct phosphorylation event on SRC3, Serine 543 phosphorylation. This phosphorylation has spatial selectivity on a genomic scale, where chromatin binding was selectively enriched at active promoter regions. This genomic preference at promoters is on contrast to total SRC3, which is mainly found at enhancers. It is likely that SRC3 and SRC3-pS543 antibodies have different sensitivities, and the level of overlap detected between these two signals is possibly an underestimate of the actual proportion of SRC3 that is phosphorylated. Relative expression levels and antibody sensitivity are likely to alter the threshold of detection in ChIP-seq experiments, forming a major source for false-negative signal. Because the strongest total SRC3 sites are enhancer-selective, whereas the strongest SRC-pS543 were mostly enriched at promoters, this genomic selectivity of phosphorylated SRC3 to promoter regions cannot be merely explained by relative expression levels or antibody sensitivity.

Because ERα typically binds enhancers (30), the determination of which ERα binding events are functionally orchestrating what genes has re-

mained a challenge in the field. Because most ERα binding events are observed within a 20-kb window from the transcription start sites of responsive genes (33), this spacing around the promoter is typically applied to provide an indication of functionality. All p160 coactivators, including SRC3, show comparable genomic features as compared with ERα and are typically found at enhancers as well (15). Because the SRC3-pS543 phosphorylation is promoter-enriched, commonly shared with ERα and induced by estradiol, this phosphorylation event could be considered as a novel ERα functionality probe, highlighting ERα complexes that are actively involved in transcriptional events at gene promoters.

Smaller previous studies on SRC3 expression and its correlations with ERα and members of the EGFR/HER family have reported varying results (11–13). We find no correlation of SRC3 with ERα but do find a correlation with HER2 and HER3. However, SRC3-pS543 does significantly correlate with ERα, potentially reflecting the role of E2/ERα in phosphorylation of SRC3. Consistent with these results was the observed correlation of SRC3-pS543 with known estrogen-regulated genes, including PR. Although previous studies have explored the influence of SRC3 expression on patient outcome as well how it may influence endocrine therapy (11–13, 34–39), the current study is the largest and most well-characterized series to date, with a long median follow-up. We find no statistically significant association between SRC3 levels and DFS and BCSS in patients with ERα-positive breast cancer treated with tamoxifen, consistent with other reports (12, 13). Of note, in those women with ERα-positive tumors not treated with tamoxifen, there is a trend to an improved outcome and survival for SRC3-positive tumors, analogous to the first report relating SRC3 and response to endocrine therapy (11). The poor outcome seen in HER2-positive/SRC3-high tumors for patients treated with tamoxifen is consistent with previously published data (11, 12). One previous study on ERα-negative tumors, which utilized automated quantitative analysis in a subgroup of 133 patients, found SRC3 associated with a poorer overall survival (38). However, in the current study of 377 ERα-negative tumors no correlations with recurrence or outcome were found for SRC3. Of note, we show a significant correlation of p-JNK and p-p38 with SRC3-pS543. These kinases have previously been described to phosphorylate SRC3-S543 (16), and activated (phosphorylated) JNK has previously be linked to endocrine therapy resistance (37) (40), as well as poor outcome in breast cancer (41). The current study linking pJNK with high SRC3-pS543 and a good prognosis group is not comparable with these previous studies for

technical and methodological reasons. In the previous study, which investigated the expression of pJNK in human breast cancer (39), differing reagents, scoring system, as well as a smaller number of cases (n = 68) was used. Furthermore, 40% of the cases were ERα negative, and in those that were ERα positive no clinicopathologic correlation was presented (39). Although the other studies either investigated the activity of JNK and not its expression in the context of breast cancers exposed to tamoxifen (37) or where levels of pJNK were assessed via immunoblotting in the context of a MCF7 breast cancer xenograft model (38).

Our study is the first to explore the clinical significance of a phosphorylated form of SRC3. SRC3-pS543 correlates with an improved DFS and BCSS for the whole cohort and is a predictor of outcome in ERα-positive breast cancer. Furthermore, in high-risk ER-positive disease it is demonstrated that SRC3-pS543 is predictive of benefit with adjuvant tamoxifen. With no benefit being seen with adjuvant tamoxifen in the presence of high SRC3-pS543, although those tumors with low SRC3-pS543 had improved outcomes with tamoxifen treatment. The lack of benefit observed in high SRC3-pS543 tumors treated with tamoxifen indicates that the transcriptional events driven by SRC3-pS543 at gene promoters of ERα responsive result in a phenotype with an excellent clinical outcome, this would be consistent with the clinicopathologic features associated with SRC3-pS543. Although insufficiency or inability to enrich at these promoters as a result of low or absent SRC3-pS543 results in a more aggressive phenotype, which can be abrogated by tamoxifen.

The patient group studied here is a well-characterized historical cohort treated with or without tamoxifen. However, estrogen withdrawal therapy using aromatase inhibitors (AI) is now a standard clinical practice in the adjuvant setting for postmenopausal breast cancer, and correlations of response to AIs with (phosphorylated) SRC3 levels need to be assessed within this setting, particularly because the oncogenicity of SRC3 appears modulated by the hormonal milieu in mouse models (42). Currently, the translational arm of the Intergroup Exemestane Study (so-called Path-IES) is exploring the potential role of SRC3 and pS543 in this context (43).

In summary, we have found a novel biomarker for ERα-positive breast cancer and provide mechanistic insights in its functional involvement in the ERα transcription complex. SRC3-pS543 phospho-specific antibodies could aid in identifying patients with a functional ERα signaling pathway, which predicts for a favorable outcome in the absence of adjuvant therapy

and where tamoxifen might better be withheld.

Material and Methods

Cell lines, plasmids and antibodies.

MCF-7 and CHO cells were from the American Type Culture Collection (ATCC), which utilises short tandem repeat profiling with no authentication being performed by authors. All experiments were performed within 10 passages from the original stock. Cell lines were grown in DMEM with 10% FCS and standard antibiotics. Wild type SRC3 and mutant S543A plasmids kindly provided by BW O'Malley (Baylor College of Medicine). The antibodies used were SRC3 (Immunohistochemistry, BD Transduction Laboratories; 611105), SRC3 (ChIP-seq experiments, SC-9119; Santa Cruz), ERα (SC-543; Santa Cruz). A rabbit polyclonal antiserum for SRC3-pS543 was generated by immunising animals with the peptide 537-LLSTLSSPGPKLDN-550, where the residue in bold is phospho-serine (Moravian Biotechnologies, Czech Republic).

(Chromatin) Immunoprecipitations

Chromatin immunoprecipitations were performed according to standard protocols (Schmidt et al., 2009). Primary breast cancer specimens and proliferation MCF-7 breast cancer cells were used. Tissue was cryosectioned in 30 slices of 30 μm, and subsequently defrosted in solution A (50 mM Hepes, 100 mM NaCl, 1mM EDTA, 0.5 mM EGTA) supplemented with 1% formaldehyde. For MCF-7 cells, formaldehyde as added to the culture medium at a final concentration of 1%. After 10 minutes of fixation, 100 mM Glycine as added, after which cells were washed in PBS in presence of Protease Inhibitor (Roche Diagnostics 11836145001) and Phosphatase Inhibitors (Roche Diagnostics: 04906837001). Tissue was homogenized, and nuclei were isolated, washed and sonicated using a Diagenode Bioruptor as described before (Zwart et al., 2013, Jansen et al., 2013). After sonication, the lysate was cleared by centrifugation. For each ChIP 100μl of Dynabeads (Invitrogen) was used, precoupled overnight with 10μg of SRC3 or SRC-pS543 antibody. Immunoprecipitation was performed overnight while rotating at 4 degrees. Subsequently, beads were washed 10 times using RIPA buffer and reverse crosslinked at 65 degrees for 6 hours. Supernatant was removed, cleaned using a phenol/chloroform column and precipitated as described before (Schmidt et al., 2009). For standard Immunoprecipitations, beads were resuspended in sample buff-

er, boiled at 95˚C for 5mins and the samples run onto 8% Polyacrylamide gel for protein analysis for S543P, Input SRC3 and Immunoprecipitated (IP) SRC3. Immunoprecipitations were performed in presence of Protease Inhibitor (Roche Diagnostics 11836145001) and Phosphatase Inhibitors (Roche Diagnostics: 04906837001). When indicated, samples were incubated with Lambda Protein Phosphatase (Millipore; cat # 14-405) for 30 min prior to ChIP. Primer sequences for QPCR analysis are in Supplementary Table S1.
For MCF-7 experiments, ~6x107 asynchronous proliferating cells were used, and two independent replicates were performed for each ChIP-seq, where only consensus peaks that were found in both experiments were considered. For tumour specimen ChIP-seq, fresh snap-frozen primary ERα-positive, HER2-negative untreated breast cancers were obtained from the Imperial College Healthcare NHS Trust Tissue Bank which has the requisite ethical approval..

Solexa sequencing and enrichment analysis
ChIP DNA was amplified as described (Schmidt et al., 2009). Sequences were generated by the Illumina Hiseq 2000 genome analyser (using 50 bp reads), and aligned to the Human Reference Genome (assembly hg19, February 2009). Enriched regions of the genome were identified by comparing the ChIP samples to mixed input using the MACS peak caller (Zhang et al., 2008) version 1.3.7.1. Total read count, percentage of aligned reads and number of peaks for each ChIP-seq is shown in Supplementary Table S2. For histone modification data, publically available MCF-7 ChIP-seq data for H3K4me1 (GEO: GSM588568), H3K4me2 (GEO: GSM822392), H3K4me3 (GEO: GSM945269) and H3K27Ac (GEO: GSM945854) was used. For ERα ChIP-seq data, peaks from (Ross-Innes et al., 2012) were used. ChIP-seq data for SRC1, SRC2 and total SRC3 were from (Zwart et al., 2011b). For heatmap visualizations, Seqminer software was used.

Motif analysis, heatmaps and genomic distributions of binding events
ChIP-seq data snapshots were generated using the Integrative Genome Viewer IGV 2.1 (www.broadinstitute.org/igv/). Motif analyses were performed through the Cistrome (cistrome.org), applying the SeqPos motif tool (He et al., 2010). The genomic distributions of binding sites were analysed using the cis-regulatory element annotation system (CEAS) (Ji et al., 2006). The genes closest to the binding site on both strands were analysed. If the binding region is within a gene, CEAS software indicates whether it is in a 5′UTR, 3′UTR,

coding exon, or an intron. Promoter is defined as 3 kb upstream from RefSeq 5′ start. If a binding site is >3 kb away from the RefSeq transcription start site, it is considered distal intergenic.

Nottingham Tenovus Primary breast cancer Series

Primary operable breast cancer cases (n = 1,650) from the Nottingham Tenovus Primary Breast Carcinoma Series was utilised as described before (Elston and Ellis, 1991, Ellis et al., 1992), supplementary table S3. Patients were under the age of 71 years (median, 55 years), diagnosed between 1986 and 1999, and treated uniformly in a single institution. Patients within the good prognosis group (Nottingham Prognostic Index (NPI) <3.4) did not receive adjuvant therapy. Pre-menopausal patients within the moderate (NPI >3.4 to <5.4) and poor (NPI >5.4) prognosis groups were candidates for chemotherapy. Conversely, postmenopausal patients with ERα positive breast cancer with moderate or poor NPI were offered hormonal therapy, while ERα-negative patients received chemotherapy. Clinical data were maintained on a prospective basis with a median follow-up of 130 months (Range 2-311 months).

Immunohistochemistry

Breast cancer tissue microarrays (TMAs) from 1,650 cases were immuno-stained with SRC3 (Dilution 1:20) and SRC3-pS543 (Dilution: 1:2000) antibodies overnight at room temperature, after antigen retrieval (citrate buffer (pH 6.0) and microwave (20 minutes at 750Watts). Negative controls were performed by omission of the primary antibody. Nuclear staining was scored based on H-score. Determination of the optimal cut-offs was performed using X-tile bioinformatics software (Yale University, USA) and according to histogram distribution of H-score. For immunohistochemistry blocking experiments, peptides were used which contained the phospho-moiety (CLLSTLS-phosphoS-PGPKLDN) or the non-phospho peptide CLLSTLSSPGPKLDN). The peptides were pre-incubated overnight at 100 fold excess over antibody prior to staining as described previously.

Statistical analysis

Data analysis was performed using SPSS (SPSS, version 17 Chicago, IL). Where appropriate, Pearson's Chi-square, Fisher's exact, Student's t and ANOVAs one-way tests were used. Cumulative survival probabilities were estimated using the Kaplan–Meier method and differences between survival rates were tested using the log-rank test. Multivariate analysis for survival

was performed using the Cox hazard model. The proportional hazards assumption was tested using standard log-log plots. Hazard ratios (HR) and 95% confidence intervals (95% CI) were estimated for each variable, with $p<0.05$ as significant. For multiple comparisons, a stringent p value (<0.001) was considered significant.

Acknowledgments
The authors thank Gordon Brown (CRI) and Arno Velds (NKI) for bioinformatics support as well as James Hadfield (CRI), Ron Kerkhoven (NKI) for Solexa sequencing, Professor Gerry Thomas, Sarah Chilcott-Burns, and Imperial College Healthcare NHS Trust, Human Biomaterials Resource Centre (Tissue Bank). In addition, the authors thank Angie Gillies (University of Leceister) and Core Facility of the Molecular Pathology Biobank of the Netherlands Cancer Institute for technical help with IHC and IHC validation experiments.

Authors' Contributions
Conception and design: W. Zwart, S. Chan, R.C. Coombes, J.S. Carroll, S. Ali, C. Palmieri; Development of methodology: W. Zwart, B. Rudraraju, T.M.A. Abdel-Fatah, O. Gojis, S. Chan, J. Shaw, R.C. Coombes, J.S. Carroll, S. Ali, C. Palmieri; Acquisition of data (provided animals, acquired and managed patients, provided facilities, etc.): W. Zwart, K.D. Flach, B. Rudraraju, T.M.A. Abdel-Fatah, D. Moore, M. Opdam, I. Hofland, S. Chan, I.O. Ellis, R.C. Coombes, C. Palmieri; Analysis and interpretation of data (e.g., statistical analysis, biostatistics, computational analysis): W. Zwart, K.D. Flach, B. Rudraraju, T.M.A. Abdel-Fatah, S. Canisius, E. Nevedomskaya, M. Opdam, M. Droog, S. Chan, J. Shaw, I.O. Ellis, R.C. Coombes, J.S. Carroll; Writing, review, and/or revision of the manuscript: W. Zwart, K.D. Flach, T.M.A. Abdel-Fatah, S. Chan, I.O. Ellis, R.C. Coombes, S. Ali, C. Palmieri; Administrative, technical, or material support (i.e., reporting or organizing data, constructing databases): B. Rudraraju, T.M.A. Abdel-Fatah, M. Opdam, S. Chan, C. Palmieri; Study supervision: W. Zwart, S. Chan, R.C. Coombes
The authors declare no conflict of interest.

References

1. Ali S, Coombes RC. Endocrine-responsive breast cancer and strategies for combating resistance. Nature Rev Cancer 2002;2:101–12.

2. York B, O'Malley BW. Steroid receptor coactivator (SRC) family: masters of systems biology. J Biol Chem 2010;285:38743–50.

3. List HJ, Lauritsen KJ, Reiter R, Powers C, Wellstein A, Riegel AT. Ribozyme targeting demonstrates that the nuclear receptor coactivator AIB1 is a ratelimiting factor for estrogen-dependent growth of human MCF-7 breast cancer cells. J Biol Chem 2001;276:23763–8.

4. Torres-Arzayus MI, Font de Mora J, Yuan J, Vazquez F, Bronson R, Rue M, et al. High tumor incidence and activation of the PI3K/AKT pathway in transgenic mice define AIB1 as an oncogene. Cancer Cell 2004;6: 263–74.

5. Kuang SQ, Liao L, Wang S, Medina D, O'Malley BW, Xu J. Mice lacking the amplified in breast cancer 1/steroid receptor coactivator-3 are resistant to chemical carcinogen-induced mammary tumorigenesis. Cancer Res 2005; 65:7993–8002.

6. Fereshteh MP, Tilli MT, Kim SE, Xu J, O'Malley BW, Wellstein A, et al. The nuclear receptor coactivator amplified in breast cancer-1 is required for Neu (ErbB2/HER2) activation, signaling, and mammary tumorigenesis in mice. Cancer Res 2008;68:3697–706.

7. Anzick SL, Kononen J, Walker RL, Azorsa DO, Tanner MM, Guan XY, et al. AIB1, a steroid receptor coactivator amplified in breast and ovarian cancer. Science 1997;277:965–8.

8. Murphy LC, Simon SL, Parkes A, Leygue E, Dotzlaw H, Snell L, et al. Altered expression of estrogen receptor coregulators during human breast tumorigenesis. Cancer Res 2000;60:6266–71.

9. Bouras T, Southey MC, Venter DJ. Overexpression of the steroid receptor coactivator AIB1 in breast cancer correlates with the absence of estrogen and progesterone receptors and positivity for p53 and HER2/neu. Cancer Res 2001;61:903–7.

10. Gojis O, Rudraraju B, Gudi M, Hogben K, Sousha S, Coombes RC, et al. The role of SRC-3 in human breast cancer. Nature Rev Clin Oncol 2010;7:83–9.

11. Osborne CK, Bardou V, Hopp TA, Chamness GC, Hilsenbeck SG, Fuqua SA, et al. Role of the estrogen receptor coactivator AIB1 (SRC-3) and HER-2/neu in tamoxifen resistance in breast cancer. J Natl Cancer Inst 2003;95: 353–61.

12. Kirkegaard T, McGlynn LM, Campbell FM, Muller S, Tovey SM, Dunne B, et al. Amplified in breast cancer 1 in human epidermal growth factor receptor–positive tumors of tamoxifen-treated breast cancer patients. Clin Cancer Res 2007;13:1405–11.

13. Dihge L, Bendahl PO, Grabau D, Isola J, Lovgren K, Ryden L, et al. Epidermal

growth factor receptor (EGFR) and the estrogen receptor modulator amplified in breast cancer (AIB1) for predicting clinical outcome after adjuvant tamoxifen in breast cancer. Breast Cancer Res Treat 2008; 109:255–62.

14. Alkner S, Bendahl PO, Grabau D, Lovgren K, Stal O, Ryden L, et al. AIB1 is a predictive factor for tamoxifen response in premenopausal women. Ann Oncol 2010;21:238–44.

15. Zwart W, Theodorou V, Kok M, Canisius S, Linn S, Carroll JS. Oestrogen receptor-co-factor-chromatin specificity in the transcriptional regulation of breast cancer. EMBO J 2011;30:4764–76.

16. Wu RC, Qin J, Yi P, Wong J, Tsai SY, Tsai MJ, et al. Selective phosphorylations of the SRC-3/AIB1 coactivator integrate genomic reponses to multiple cellular signaling pathways. Mol Cell 2004;15:937–49.

17. Oh AS, Lahusen JT, Chien CD, Fereshteh MP, Zhang X, Dakshanamurthy S, et al. Tyrosine phosphorylation of the nuclear receptor coactivator AIB1/SRC-3 is enhanced by Abl kinase and is required for its activity in cancer cells. Mol Cell Biol 2008;28:6580–93.

18. Li C, Liang YY, Feng XH, Tsai SY, Tsai MJ, O'Malley BW. Essential phosphatases and a phospho-degron are critical for regulation of SRC-3/AIB1 coactivator function and turnover. Mol Cell 2008;31:835–49.

19. Xu J, Li Q. Review of the in vivo functions of the p160 steroid receptor coactivator family. Mol Endocrinol 2003;17:1681–92.

20. Schmidt D, Wilson MD, Spyrou C, Brown GD, Hadfield J, Odom DT. ChIPseq: using high-throughput sequencing to discover protein-DNA interactions. Methods 2009;48:240–8.

21. Zwart W, Koornstra R, Wesseling J, Rutgers E, Linn S, Carroll JS. A carrierassisted ChIP-seq method for estrogen receptor-chromatin interactions from breast cancer core needle biopsy samples. BMC Genomics 2013; 14:232.

22. Jansen MP, Knijnenburg T, Reijm EA, Simon I, Kerkhoven R, Droog M, et al. Hallmarks of aromatase inhibitor drug resistance revealed by epigenetic profiling in breast cancer. Cancer Res 2013;73:6632–41.

23. Zhang Y, Liu T, Meyer CA, Eeckhoute J, Johnson DS, Bernstein BE, et al. Model-based analysis of ChIP-Seq (MACS). Genome Biol 2008;9: R137.

24. Ross-Innes CS, Stark R, Teschendorff AE, Holmes KA, Ali HR, Dunning MJ, et al. Differential oestrogen receptor binding is associated with clinical outcome in breast cancer. Nature 2012;481:389–93.

25. He HH, Meyer CA, Shin H, Bailey ST, Wei G, Wang Q, et al. Nucleosome dynamics define transcriptional enhancers. Nature Genetics 2010;42: 343–7.

26. Ji X, Li W, Song J, Wei L, Liu XS. CEAS: cis-regulatory element annotation sys-

tem. Nucleic Acids Res 2006;34(Web Server issue):W551–4.
27. Elston CW, Ellis IO. Pathological prognostic factors in breast cancer. I. The value of histological grade in breast cancer: experience from a large study with long-term follow-up. Histopathology 1991;19:403–10.
28. Ellis IO, Galea M, Broughton N, Locker A, Blamey RW, Elston CW. Pathological prognostic factors in breast cancer. II. Histological type. Relationship with survival in a large study with long-term follow-up.
Histopathology 1992;20:479–89.
29. Madak-Erdogan Z, Charn TH, Jiang Y, Liu ET, Katzenellenbogen JA, Katzenellenbogen BS. Integrative genomics of gene and metabolic regulation by estrogen receptors alpha and beta, and their coregulators. Mol Syst Biol 2013;9:676.
30. Carroll JS, Liu XS, Brodsky AS, Li W, Meyer CA, Szary AJ, et al. Chromosome-wide mapping of estrogen receptor binding reveals long-range regulation requiring the forkhead protein FoxA1. Cell 2005;
122:33–43.
31. Zwart W, Theodorou V, Carroll JS. Estrogen receptor-positive breast cancer: a multidisciplinary challenge. Wiley Interdiscip Rev Syst Biol Med 2011;3: 216–30.
32. Tan SK, Lin ZH, Chang CW, Varang V, Chng KR, Pan YF, et al. AP-2gamma regulates oestrogen receptor-mediated long-range chromatin interaction and gene transcription. EMBO J 2011;30:2569–81.
33. Fullwood MJ, Liu MH, Pan YF, Liu J, Xu H, Mohamed YB, et al. An oestrogen-receptor-alpha-bound human chromatin interactome. Nature 2009;462:58–64.
34. Bautista S, Valles H, Walker RL, Anzick S, Zeillinger R, Meltzer P, et al. In breast cancer, amplification of the steroid receptor coactivator gene AIB1 is correlated with estrogen and progesterone receptor positivity. Clin Cancer Res 1998;4:2925–9.
35. List HJ, Reiter R, Singh B, Wellstein A, Riegel AT. Expression of the nuclear coactivator AIB1 in normal and malignant breast tissue. Breast Cancer Res Treat 2001;68:21–8.
36. Hudelist G, Czerwenka K, Kubista E, Marton E, Pischinger K, Singer CF. Expression of sex steroid receptors and their co-factors in normal and malignant breast tissue: AIB1 is a carcinoma-specific co-activator. Breast Cancer Res Treat 2003;78:193–204.
37. Thorat MA, Turbin D, Morimiya A, Leung S, Zhang Q, Jeng MH, et al. Amplified in breast cancer 1 expression in breast cancer. Histopathology 2008;53:634–41.
38. Harigopal M, Heymann J, Ghosh S, Anagnostou V, Camp RL, Rimm DL. Estrogen receptor co-activator (AIB1) protein expression by automated quantitative analysis (AQUA) in a breast cancer tissue microarray and association with patient outcome. Breast Cancer Res Treat 2009;115:77–85.

39. Iwase H, Omoto Y, Toyama T, Yamashita H, Hara Y, Sugiura H, et al. Clinical significance of AIB1 expression in human breast cancer. Breast Cancer Res Treat 2003;80:339–45.
40. Schiff R, Reddy P, Ahotupa M, Coronado-Heinsohn E, Grim M, Hilsenbeck SG, et al. Oxidative stress and AP-1 activity in tamoxifen-resistant breast tumors in vivo. J Natl Cancer Inst 2000;92:1926–34.
41. Yeh YT, Hou MF, Chung YF, Chen YJ, Yang SF, Chen DC, et al. Decreased expression of phosphorylated JNK in breast infiltrating ductal carcinoma is associated with a better overall survival. Int J Cancer 2006;118:2678–84.
42. Torres-Arzayus MI, Zhao J, Bronson R, Brown M. Estrogen-dependent and estrogen-independent mechanisms contribute to AIB1-mediated tumor formation. Cancer Res 2010;70:4102–11.
43. Viale G, Speirs V, Bartlett JM, Mousa K, Kalaitzaki E, Palmieri C , et al. Prognostic and predictive value of IHC4 and ER in the Intergroup Exemestane Study (IES). Ann Oncol 2013;24(Suppl 3):iii37.

Table 1*: Patient characteristics and tumor biomarkers and correlation SRC3 and SRC3-pS543*
See online supplemental information

Supplementary information

Supplementary Figure 1-14 and table 1-6
See online supplemental information

Table 2*: Multivariate analysis using Cox regression analysis confirms that SRC3-pS543 protein expression is an independent prognostic factor for both DFS and BCSS*

	BCSS at 10 years		DFS at 10 years	
Variable	**HR (CI 95%)**	***P***	**HR (CI 95%)**	***P***
S543 (low expression)	1.6 (1.1–2.5)	0.024*	1.4 (1.0–1.9)	0.038*
Tumor size	1.1 (1.0–1.3)	0.056	1.1 (1.0–1.2)	0.017^{-7a}
Grade		0.018*		0.933
G1	1.0		1.0	
G2	1.4 (1.3–3.1)		0.98 (0.7–1.4)	
G3	2.1 (2.6–5.7)		1.03 (1.2–2.0)	
Lymph node stage		9.6×10^{-11}*		1.6×10^{-10}*
Negative	1		1	
Positive (1–3 nodes)	1.7 (1.3–2.3)		1.4 (1.1–1.8)	
Positive (>3 nodes)	3.6 (2.5–5.3)		3.2 (2.3–4.4)	
Endocrine therapy (no)	1.1 (0.8–1.4)	0.661	0.9 (0.7–1.2)	0.565
Chemotherapy (no)	1.2 (0.9–1.7)	0.259	1.3 (1.0–1.7)	0.03
Bcl2 expression (positive)	0.4 (0.3–0.6)	6.8×10^{-8}*	0.5 (0.4–0.7)	9.2×10^{-7}*
Ki67 expression (high)	1.5 (1.1–2.2)	0.022*	1.3 (1.0–1.7)	0.093*
ER expression (negative)	1.5 (1.1–2.1)	0.016*	1.4 (1.0–1.8)	0.036*
HER2 (overexpression)	1.7 (1.2–2.4)	0.002*	0.7 (0.5–1.0)	0.03*

**Statistically significant*